RAPID COMMUNICATIONS IN MASS SPECTROMETRY
Rapid Commun. Mass Spectrom. **14**, 551–563 (2000)

Comparative analysis of ceramide structural modification found in fungal cerebrosides by electrospray tandem mass spectrometry with low energy collision-induced dissociation of Li^+ adduct ions

Steven B. Levery[1]*, Marcos S. Toledo[2], Ron Lou Doong[1], Anita H. Straus[2] and Helio K. Takahashi[2]

[1]The Complex Carbohydrate Research Center and Department of Biochemistry and Molecular Biology, University of Georgia, 220 Riverbend Road, Athens, GA 30602-7229, USA
[2]Department of Biochemistry, Universidade Federal de São Paulo/Escola Paulista de Medicina, Rua Botucatu 862, 04023-900, São Paulo, SP, Brasil

Fungal cerebrosides (monohexosylceramides, or CMHs) exhibit a number of ceramide structural modifications not found in mammalian glycosphingolipids, which present additional challenges for their complete characterization. The use of Li^+ cationization, in conjunction with electrospray ionization mass spectrometry and low energy collision-induced dissociation tandem mass spectrometry (ESI-MS/CID-MS), was found to be particularly effective for detailed structural analysis of complex fungal CMHs, especially minor components present in mixtures at extremely low abundance. A substantial increase in both sensitivity and fragmentation was observed on collision-induced dissociation of $[M + Li]^+$ *versus* $[M + Na]^+$ of the same CMH components analyzed under similar conditions. The effects of particular modifications on fragmentation were first systematically evaluated by analysis of a wide variety of standard CMHs expressing progressively more functionalized ceramides. These included bovine brain galactocerebrosides with non-hydroxy and 2-hydroxy fatty *N*-acylation; a plant glucocerebroside having (*E*/*Z*)-Δ^8 in addition to (*E*)-Δ^4 unsaturation of the sphingoid base; and a pair of fungal cerebrosides known to be further modified by a branching 9-methyl group on the sphingoid moiety, and to have a 2-hydroxy fatty *N*-acyl moiety either fully saturated or (*E*)-Δ^3 unsaturated. The method was then applied to characterization of both major and minor components in CMH fractions from a non-pathogenic mycelial fungus, *Aspergillus niger;* and from pathogenic strains of *Candida albicans* (yeast form); three *Cryptococcus* spp. (all yeast forms); and *Paracoccidioides brasiliensis* (both yeast and mycelium forms). The major components of all species examined differed primarily (and widely) in the level of 2-hydroxy fatty *N*-acyl Δ^3 unsaturation, but among the minor components a significant degree of additional structural diversity was observed, based on differences in sphingoid or *N*-acyl chain length, as well as on the presence or absence of the sphingoid Δ^8 unsaturation or 9-methyl group. Some variants were isobaric, and were not uniformly present in all species, affirming the need for MS/CID-MS analysis for full characterization of all components in a fungal CMH fraction. The diversity in ceramide distribution observed may reflect significant species-specific differences among fungi with respect to cerebroside biosynthesis and function.

Received 21 December 1999; Revised 28 January 2000; Accepted 31 January 2000

Glycosphingolipids (GSLs), which are the glycosides of *N*-acylsphingosine, or ceramide (Cer), are a structurally and functionally diverse group of molecules ubiquitously distributed among all eukaryotes.[1] Certain marine invertebrates, plants, and fungi, including many mycopathogens, express monohexosylceramides (cerebrosides, or CMHs) with distinctive structural modifications of the ceramide moiety not found in mammalian GSLs.[2–15] These modifications include additional sites of unsaturation, which provide possibilities for structural heterogeneity in addition to those derived from variations in sphingosine and fatty *N*-acyl hydroxylation and chain length, and in the monosaccharide moiety. In the case of fungi, such additional variations may have functional importance in growth, life cycle, morphogenesis, and host-pathogen interactions. However, although a number of suggestive phenomena and correlations have been observed with fungal cerebrosides *in vitro*,[16–22] very little is known about their true functions, biosynthesis, or metabolic fate *in vivo*. Understanding these processes will be facilitated by the development of routine and sensitive protocols for both structural and quantitative analysis of fungal cerebrosides, including biosynthetic intermediates

*Correspondence to: S. B. Levery, The Complex Carbohydrate Research Center, University of Georgia, 220 Riverbend Road, Athens, GA 30602-7229, USA.
E-mail: leverysb@ccrc.uga.edu
Contract/grant sponsor: FAPESP, Brasil. Contract/grant sponsor: CNPq, Brasil. Contract/grant sponsor: PRONEX, Brasil. Contract/grant sponsor: Noese Technologies, Inc. Contract/grant sponsor: National Institutes of Health; Contract/grant number: P41 RR05351.

and metabolic products which may be present in very low abundance. Such methods will be invaluable for correlating the expression of cerebroside structural variants with different species, strains, or culture conditions; and with fungal growth, differentiation, morphogenesis, or pathogenicity; as well as for detection and elucidation of previously unknown structural analogs.

Mass spectrometry has long been a crucial tool for the structural analysis of GSLs.[23–27] Although the glycan moiety is amenable to sequencing by a wide variety of high and low energy mass spectrometric techniques, those involving high energy collision-induced dissociation (CID) have generally been the most useful for elucidating details of ceramide structure without derivatization or degradation[25,26,28] (rather than just providing molecular mass profiles). Applications of high energy tandem CID-MS without derivatization have included characterization of highly functionalized cerebrosides as typically found in fungi.[11] Gu *et al.*[29] analyzed protonated ceramides and a fungal cerebroside by low energy tandem quadrupole $^+$ESI-MS/CID-MS, but provided almost no interpretive details for the latter spectrum, as their principal interest was in ceramide profiling of lipid mixtures by parent ion scanning from common fragment ions. In our hands, tandem quadrupole $^+$ESI-MS/CID-MS of sodiated underivatized cerebrosides was found to be useful for verifying carbon and unsaturation numbers for the acyl and sphingosine moieties of fungal cerebrosides,[22,36] but fragments specifying the locations of double bonds, methyl groups, and other functional groups were not reliably produced under low energy conditions. In addition, it was found to be impractical to obtain even minimal CID data on minor components of CMH mixtures with reasonable expenditure of material. The use of Li^+ adduction, as recommended by Ann and Adams,[30,31] appears to be superior for these purposes, and has been applied at high collision energies to GSLs, including cerebrosides from mammals,[30,31] plants[32] and fungi;[14] and at medium energies (400 eV in an orthogonal sector-TOF hybrid), to cerebrosides and other GSLs from mammals.[33] However, as far as we are aware, it has not been applied to complex cerebrosides, such as those found in fungi, under low energy CID conditions.

The following results show that considerable improvement in sensitivity and information content can be conveniently obtained from CID-MS of Li^+ adducts of a wide variety of CMH structures without the use of high collision energies. The influence of particular modifications on fragmentation was first systematically evaluated by analysis of a panel of known mammalian, plant, and fungal CMHs expressing progressively more functionalized ceramides. Subsequent application to a wider variety of both major and minor components of fungal cerebrosides, most of which had not been previously characterized, pointed to interesting differences in CMH biosynthesis among various species, which may furthermore reflect significant diversity with respect to glycosphingolipid function in fungi.

EXPERIMENTAL

Bovine brain galactocerebrosides (Type II, containing 98% non-hydroxy fatty acylation, **B1**; Type I, containing 98% 2-hydroxy fatty acylation, **B2**) were purchased from Sigma (St. Louis, MO, USA); glucocerebroside from soybean (*Glycine max*) (**S1**) was purchased from Matreya, Inc. (Pleasant Gap, PA, USA). Isolation of the glucocerebrosides of yeast and mycelium forms of the thermally dimorphic mycopathogen *Paracoccidioides brasiliensis* (Pb18) (**F1, F8**, respectively) and the galactocerebroside of pathogenic *Aspergillus fumigatus* (ATCC strain 9197) (**F2**) have been described previously.[22] The three fungal cerebrosides used as standards were previously characterized by methods which included low energy $^+$ESI-MS/CID-MS of their Na^+ adducts and NMR spectroscopy.[22] Cultures of yeast forms of *Cryptococcus neoformans* (512VFSB), *Cr. laurentii* (40043), and *Cr. albidus* (40077); the yeast form of *Candida albicans* (ATCC 10231); and mycelia of *A. niger* (isolated from peanut, gift of Dr. Ron Clay) were grown on YPD medium; and their cerebrosides (**F3–F7**, respectively) extracted and purified by similar methods.[22] The *Cryptococcus* strains were all provided by Dr. Olga F. Gompertz (Universidade Federal de São Paulo/Escola Paulista de Medicina).

ESI-MS and tandem ESI-MS/CID-MS were performed in positive ion mode on a PE-Sciex (Concord, Ontario, Canada) API-III spectrometer, with a standard IonSpray source, using direct infusion (3–5 μL/min) of CMH samples dissolved (~20 ng/μL) in 100% MeOH. Under these conditions, only sodiated molecular ion adducts were normally observed in $^+$ESI-MS in the absence of additives. Appropriate amounts of Li^+ were determined empirically in $^+$ESI-MS profile mode (orifice-to-skimmer voltage (OR), 120–160 V; Ionspray voltage, 5 kV; interface temperature, 45 °C), by addition of a solution of LiI (10 mM) in MeOH until the observed ratio of Li^+ to Na^+ molecular ion was >95:5 (the final concentration of LiI was generally 2–3 mM). For $^+$ESI-MS/CID-MS experiments, the OR was set to 120 V, the collision gas was argon (collision gas thickness (CGT) = 380–400 [$\times 10^{12}$ molecules/cm^2]), and collision energy was 80 eV. Other parameters were set to achieve a peak width at half height of 0.6–0.7 Th (measured at *m/z* 332), deemed sufficient to assign nominal masses to all peaks in the mass range of interest. The mass range *m/z* 50–800 was scanned in *m/z* 0.2 steps, with a dwell time of 5 ms (2.5 ms for minor components), giving a total cycle time of 19 s (or 9.5 s). In general, spectra represent summations of 5–10 scans for single analyzer profiles, and 10–30 scans for CID experiments (50–100 for minor components), unless otherwise indicated. Fragment nomenclature is after Costello *et al.*[25,28,34] as modified and expanded by Adams and Ann[26] (see Scheme 2).

RESULTS

General observations

Li^+ complexation was promoted by successive additions of LiI to cerebrosides dissolved in pure MeOH until the Na^+ adducts normally present were substantially replaced (>95%), as observed by $^+$ESI-MS profiling of the molecular ion region. This was achieved at LiI concentrations of 2–3 mM, without substantial reduction in the overall molecular ion signal until this amount was exceeded. The effect of complexation with Li^+ *versus* Na^+ in $^+$ESI-MS/CID-MS was a general increase in signal from product ions by almost an order of magnitude under identical conditions of analysis. These observations are similar but not identical to those of Olling *et al.*,[33] who used a different instrument (sector-TOF hybrid; 400 eV lab frame collision energy) and infusion solvent for their experiments. In general, in our experiments, spectral resolution was sacrificed somewhat to

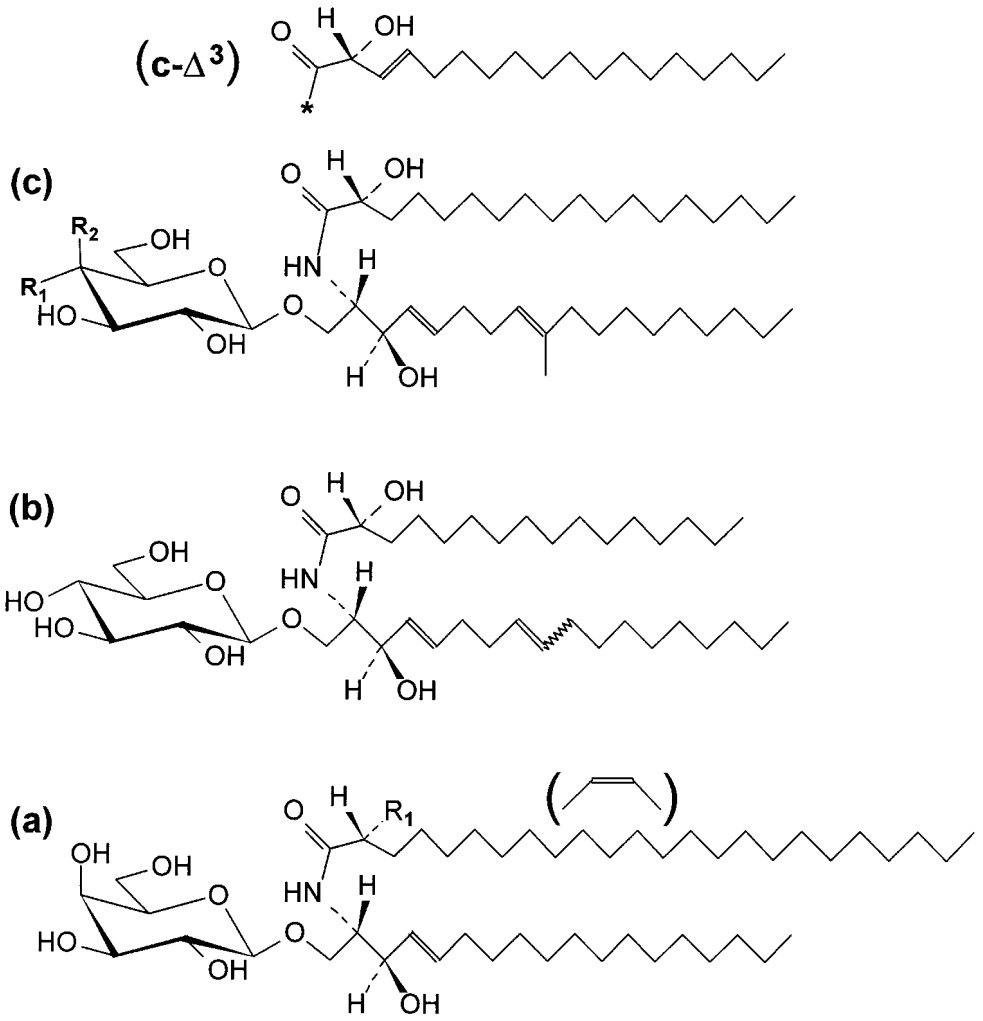

Scheme 1. Representative structures of cerebrosides used in this study: (a) Bovine brain galactocerebroside (e.g., compounds **B1a–B2c**) with non-hydroxy (R_1 = H) or 2′-hydroxy (R_1 = OH) fatty *N*-acylation; mid-chain (*Z*) unsaturation of unspecified location in parenthesis; (b) soybean glucocerebroside (e.g., compound **S1**) with 2′-hydroxy fatty *N*-acylation and additional (*E*/*Z*)-Δ^8 unsaturation of sphingoid; (c) fungal cerebrosides (e.g., compounds **F1a, F2a**) with 2′-hydroxy fatty *N*-acylation, sphingoid 9-methyl group and (*E*)-Δ^8 unsaturation, and, in some cases, additional (*E*)-Δ^3 unsaturation of fatty acid (**c**-Δ^3); monosaccharide may be either a glucosyl (R_1 = OH; R_2 = H; **F1a**) or a galactosyl (R_1 = H; R_2 = OH; **F2a**) residue.

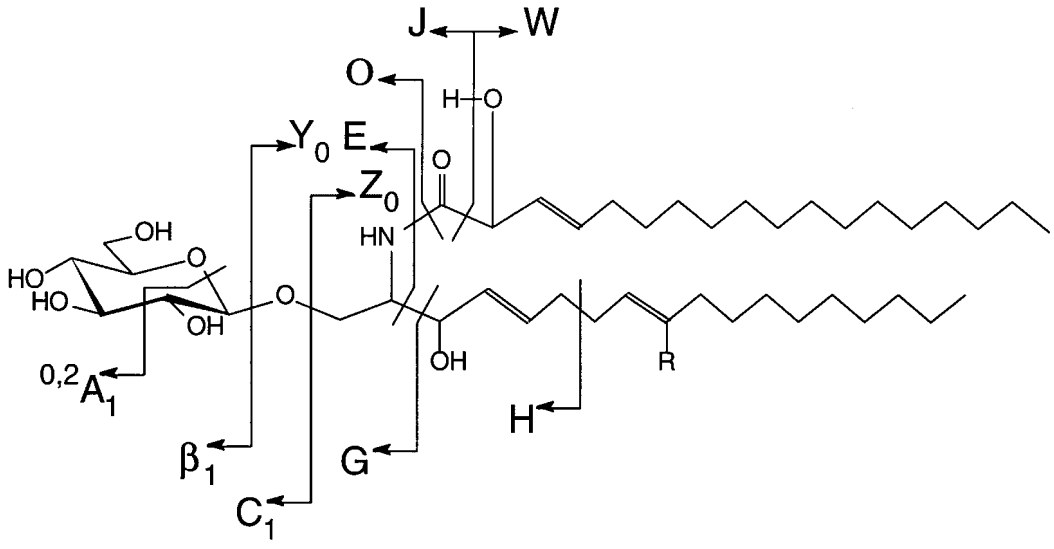

Scheme 2. Fragmentation of a cerebroside with nomenclature of Costello *et al.*[25,28,34] as modified by Adams and Ann.[26]

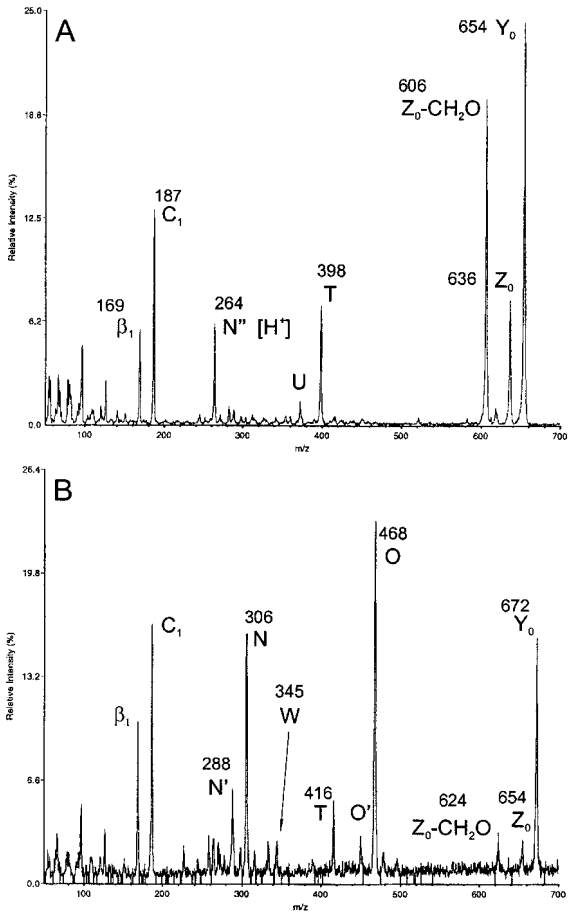

Figure 1. Comparison of tandem $^+$ESI-MS/CID-MS product ion spectra from $[M + Li]^+$ of standard bovine brain cerebrosides (Cer fatty acid + sphingosine composition in parentheses). (a) Bovine brain GalCer **B1a**, *m/z* 816 (24:1 + d18:1) and (b) bovine brain GalCer **B2b**, *m/z* 834 (h24:0 + d18:1).

achieve greater sensitivity. Although the ultimate sensitivity of analysis was not evaluated, it should be noted that acceptable results could be obtained on the major components of the fungal CMH fractions at analyte concentrations at least an order of magnitude lower than the 20 ng/μL used for this study. Total analyte concentrations were kept rather high so that CID data on minor components, some present in abundances ~1% that of the major components, could also be collected. To insure that CID data on such minor components would include reliable *m/z* assignments of as many low abundance fragments as possible, considerable oversampling was generally employed with respect to number of scans accumulated.

In order to characterize systematically the specific effects of various structural modifications on the fragmentation behavior of cerebrosides in low energy $^+$ESI-MS/CID-MS, a number of known cerebrosides having progressively more functionalized ceramide moieties were analyzed as their Li^+ adducts. These included selected major $[M + Li]^+$ species in the spectra of galactocerebrosides from bovine brain, which have 'typical' mammalian ceramides containing 4-sphingenine (d18:1) in combination with non-hydroxylated fatty acids (**B1a, B1b**) or 2-hydroxy fatty acids (**B2a, B2b, B2c**); a plant glucocerebroside having (*4E,8E* + *8Z*)-4,8-sphingadienine (d18:2) with 2-hydroxyhexadecanoate (**S1**)[7]; and the major components of two fungal cerebrosides characterized by a (*4E,8E*)-9-methyl-4,8-sphingadienine (d19:2) base in combination with either *N*-2′-hydroxyoctadecanoate (**F1a**) or *N*-(*E*)-2′-hydroxy-3′-octadecenoate (**F2a**). Following observation of fragmentation patterns for Li^+ adducts of such structurally modified cerebrosides, the method was then applied to the analysis of other fungal cerebrosides (**F3–F8**), all but one of which had either not been previously characterized or had been incorrectly or incompletely characterized.

Standard bovine brain cerebrosides

Initial comparison of $^+$ESI-MS/CID-MS product ion spectra from two types of bovine brain galactocerebrosides, which differ primarily in the absence (**B1a, B1b**) or presence (**B2a, B2b, B2c**) of fatty *N*-acyl 2′-hydroxylation (Scheme 1 (a); R_1 = H or OH, respectively), demonstrated that the additional 2′-hydroxyl group already exerts a major directing effect on fragmentation, in particular promoting highly abundant product ions from loss of the acyl group (O and N [$\equiv Y_0$/O] fragments; see Scheme 2) ions which are barely or not observed at all for the non-2′-hydroxylated analogs under these conditions (cf. Figs 1(a)(b); Table 1). A similar observation was obtained by Ann and Adams[31] for Li^+ adducts of 2′-hydroxyl *versus* non-2′-hydroxyl free ceramides analyzed by high energy CID (constant B/E ratio scanning). However, a number of other primary or secondary fragments (J,J′,O′,N′,N″,N′–CH_2O) are more abundant or newly observable for 2′-hydroxyl GalCers at lower energies (see Table 1), including aldehydes (designated 'W' Scheme 2) produced by favored cleavage of the 2′-hydroxy fatty acyl C_1–C_2 bond accompanied by transfer or loss of the 2′-hydroxyl proton (*m/z* 343, 345, 261 for **B2a, B2b**, and **B2c**, respectively). Some, but not all, of these fragments were obtained by Olling *et al.*[33] from a lithiated CMH having 2′-hydroxyhexadecanoic acid (an analogous aldehyde ion can be observed in their spectrum at *m/z* 233, although its possible origin was not discussed). Concomitant decreases in abundance of the Z_0, Z_0–CH_2O, T, U, and non-lithiated N″ (*m/z* 264) were also observed with 2′-hydroxyl *versus* non-2′-hydroxyl ceramides. The presence or absence of mid-chain (*Z*)-unsaturation of the *N*-acyl group (**B1a** vs. **B1b; B2a** vs. **B2b**) appeared to have no major influence on the fragmentation at these energies.

Standard plant cerebroside

The soybean glucocerebroside (**S1**) yielded essentially a single lithium adduct ion at *m/z* 720 (not shown); a CID product spectrum acquired from this ion is reproduced in Fig. 2(a). In contrast to mid-chain (*Z*)-unsaturation of the *N*-acyl group, introduction of a Δ^8 unsaturation into the sphingoid alkyl chain (Scheme 1 (b)) did have some notable effects, mainly ascribable to promotion of the charge remote allylic cleavages at C_2–C_3 (G) and C_6–C_7 (H). The G and H type cleavages are apparently not observed directly at these energies, but in conjunction with either dehydration (e.g., H′ at *m/z* 536), or other cleavages, such as Z_0 (to produce T [$\equiv Z_0$/G] and Z_0/H ions, *m/z* 304 and 374, respectively), or both (Z_0/H′). The Z_0′ fragment is barely detectable at *m/z* 522. Although not apparent from the CID spectrum of **S1**, because the N and T fragments are isobaric at *m/z* 304 (Table 1), the T fragment increases markedly in abundance to become the base peak for compounds containing this modification, while the relative abundance of the N

Table 1. $^{+}$ESI-MS/CID-MS data (all fragments •Li^{+} except where noted) for galactocerebrosides from bovine brain (Type II, B1a, B1b; Type I, B2a, B2b, B2c); glucocerebroside from soybean (S1); *P. brasiliensis* yeast form glucocerebroside (major component, F1a); and *A. fumigatus* galactocerebroside (major component, F2a); with proposed interpretations of fragments (all values nominal, monoisotopic *m/z*). Fragment nomenclature is after Costello *et al.*[25,28,34] as modified and expanded by Adams and Ann[26] (see Scheme 2). 3–5 most abundant fragments in each spectrum are in boldface

	B1a	**B1b**	**B2a**	**B2b**	**B2c**	**S1**	**F1a**	**F2a**
Fatty acid:	24:1	24:0	h24:1	h24:0	h18:0	h16:0	h18:0	h18:1
Sphingosine:	d18:1	d18:1	d18:1	d18:1	d18:1	d18:2	d19:2	d19:2
M	816	818	832	834	750	720	762	760
Y_0	**654**	**656**	**670**	**672**	**588**	**558**	600	598
Z_0	636	638	652	654	570	540	582	580
$Z_0'(\equiv Z_0-H_2O$	618[a]	—	—	636[a]	—	—	564	562
H′ ($\equiv$ H–H_2O	—	—	—	—	—	536	564	562
Z_0-CH_2O	**606**	**608**	622	624	540	510	552	550
J ($\equiv$ M–acyl C_2-C_ω)	—	—	496	496	496[a]	494	508	508
J′ ($\equiv$ J–H_2O)	—	—	478	478	478[a]	476	490	490
O ($\equiv$ M–acyl)	—	—	**468**	**468**	**468**	**466**	**480**	**480**
O′ ($\equiv$ M–acyl-H_2O)	—	—	450	450	450	448	462	462
Z_0/H	—	—	—	486[a]	—	374	402	400
Z_0/H′ ($\equiv Z_0$/H–H_2O)	—	—	—	468[b]	—	356	384	382
Z_0/H″ ($\equiv Z_0$/H–$2H_2O$)	—	—	—	450[b]	—	—	—	364
S ($\equiv Y_0$/G)	—	—	—	—	348[a]	320	348	346
T ($\equiv Z_0$/G)	398	400	414	416	332	**304**	**332**	**330**
N ($\equiv Y_0$/O)	—	—	**306**	**306**	**306**	304	318	318
T′ ($\equiv$ T–H_2O)	—	—	—	—	314[a]	286[b]	314[a]	312
U ($\equiv$ T–C_2H_2)	372	374[a]	388[a]	390[a]	306[b]	278	306	304[a]
N′	288	288	288	288	288	286	300	300
N″ [Li^+]	270[a]	—	270	270	270	268	282	282
N″ [H^+]	264	264	264	264	264	262[a]	—	—
N′–CH_2O	258[a]	—	258	258	258	256	270	270
W (acyl C_2-C_ω)	—	—	343	345	261	233	261	259
E	—	—	228	228	228	228	228	228
C_1	**187**	**187**	**187**	**187**	**187**	**187**	**187**	**187**
β_1	169	169	**169**	**169**	**169**	**169**	**169**	**169**
$^{0,2}A_1$	127	127	127	127	127	127	127	127
$^{0,2}A_1$–CH_2O	97	97	97	97	97	97	97	97

[a] Very weak.
[b] Probably does not contribute significantly to abundance of this fragment (isobaric with more abundant fragment in spectrum).

fragment decreases (as shown by results with fungal cerebrosides discussed in more detail below). Some fragments were difficult to assign, but in a number of cases their origins were clarified by subsequent comparison with the results from fungal cerebrosides (see below). The T, N, O (*m/z* 466), W (*m/z* 233), and other fragments were all consistent with the expected h16:0/d18:2 fatty acyl/sphingoid composition for this cerebroside (compare also the preliminary results of Sullards *et al.*[32] obtained with high energy tandem CID-MS).

Standard fungal cerebrosides

An essential difference between fungal and plant cerebrosides appears to be the addition of a branching 9-methyl group to the sphingadienine base, resulting in an increase of 14 Th for a fungal homolog having the same fatty acid. A second modification, found so far only in cerebrosides from Euascomycetes, is an additional (*E*)-Δ^3 unsaturation of the 2′-hydroxy fatty *N*-acyl group. For the previously characterized glucocerebroside from yeast forms of *P. brasiliensis* containing primarily 2′-hydroxyoctadecanoate (**F1a**; Scheme 1 (c); R_1 = OH, R_2 = H), the major $[M + Li]^+$ was observed at *m/z* 762, while for a galactocerebroside from *A. fumigatus* containing primarily (*E*)-2′-hydroxy-3′-octadecenoate (**F2a**; Scheme 1 [c-Δ^3]; R_1 = H, R_2 = OH), the major $[M + Li]^+$ was observed at *m/z* 760. The values were consistent with those for $[M + Na]^+$ previously observed for these compounds at *m/z* 778 and 776, respectively.[22]

A CID product ion spectrum acquired by selection of $[M + Li]^+$ of the *P. brasiliensis* yeast form glucocerebroside (**F1a**) is reproduced in Fig. 2(b). In comparison with a spectrum derived from the corresponding $[M + Na]^+$,[22] the major ions (β_1, C_1, T, and O) are observed in comparable relative abundance, but the overall signal-to-noise is far superior in the $[M+Li]^+$ spectrum. More significantly, the spectrum derived from the $[M + Li]^+$ adduct is considerably enriched in the abundance of minor fragments providing additional structural information, as observed above for the bovine brain and plant cerebrosides with 2-hydroxy *N*-acylation. Observable in Fig. 2(b) is a full suite of N, N′, and N″ fragments, as well as a number of others, which were not reliably produced from the $[M + Na]^+$ adduct.[22]

As might be expected, the spectrum is very similar in character to that of **S1**, differing mainly by increments of 14 Th for any fragment retaining the sphingadienine 9-methyl group and 28 Th for any fragment retaining the *N*-2′-hydroxy acyl group. Fragments resulting only from loss of the monosaccharide moiety, such as Y_0, Z_0, and Z_0-CH_2O, differed by 42 Th. Having the CID spectrum of **S1** in hand thus aided assignment of a number of fragments (summarized in Table 1) whose origins might otherwise be ambiguous. The incremental differences allowed clear

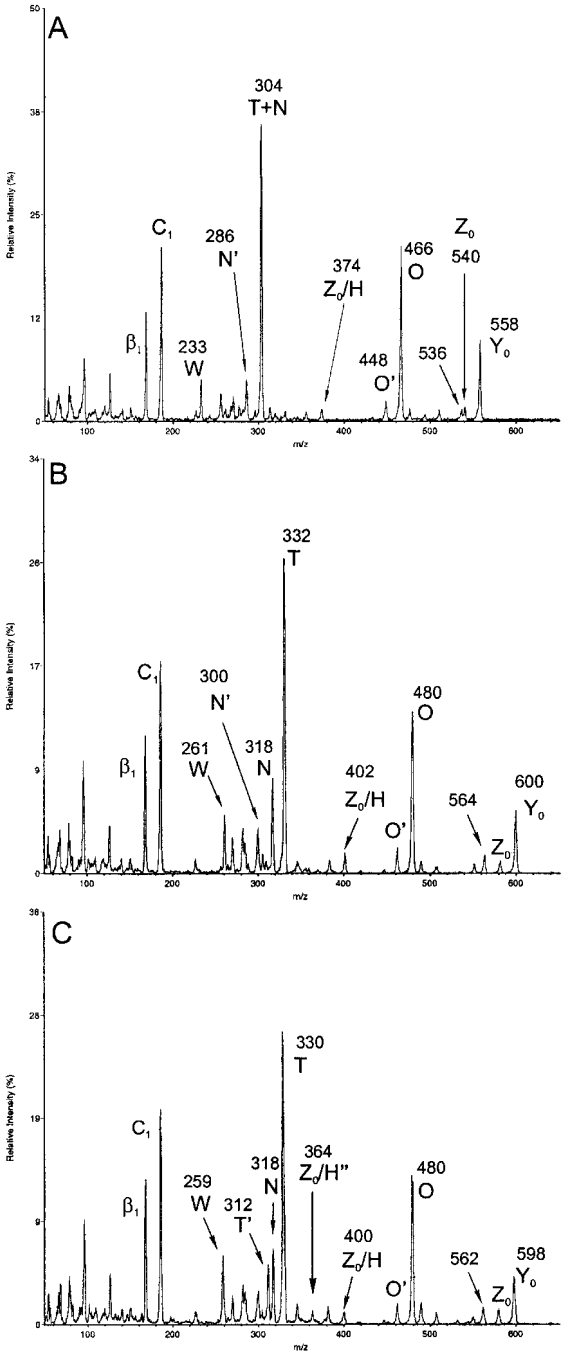

Figure 2. Comparison of tandem $^{+}$ESI-MS/CID-MS product ion spectra from $[M + Li]^+$ of standard soybean and fungal cerebrosides. (a) Soybean GlcCer **S1**, *m/z* 720 (h16:0 + d18:2); (b) *P. brasiliensis* yeast form GlcCer **F1a**, *m/z* 762 (h18:0 + d19:2); and (c) *A. fumigatus* GalCer **F2**, *m/z* 760 (h18:1 + d19:2).

observation of the increased abundance of the T relative to the N and O fragments in ceramides with a 4,8-sphingadienine base (it is doubtful this effect arises solely from the additional 9-methyl group).

An interesting ambiguity concerned the fragment at *m/z* 564, the mass of which would be consistent with assignment as either Z_0' or H′ for this compound. From the low abundance of the Z_0' relative to the H′ fragment in the spectrum of **S1**, it might be expected that most of the abundance at *m/z* 564 in this case is also from H′. However, this pattern was not consistently apparent in spectra of other fungal cerebrosides where Z_0' and H′ appeared at different *m/z*. The reason for this is unclear, but may have to do with the relative ease of dehydration of fragments containing a 2′-hydroxy fatty acyl group with versus without the Δ^3 unsaturation (see below).

A CID product ion spectrum acquired by selection of $[M + Li]^+$ of the *A. fumigatus* galactocerebroside (**F2a**) is reproduced in Fig. 2(c). The effects of the Δ^3 unsaturation of the 2′-hydroxy fatty acyl group can be clearly observed from comparison of this spectrum with that of **F1a** (Fig. 2(b)). As expected, all ions containing the fatty acyl group are decremented by 2 Th relative to those in the spectrum of **F2a**. From *m/z* 462 to 598, the spectrum is comparable to that produced by high energy FAB-CID-MS (with constant B/E ratio scanning) of products of $[M + Li]^+$ of an identical glucocerebroside from the fungus *Fusarium solani*.[14] However, numerous fragments are observable between *m/z* 602 and 730 in the high energy CID spectrum,[14] but not in the low energy spectrum. Further comparisons at the low mass end are not possible, since the *F. solani* glucocerebroside CID spectrum was truncated at *m/z* 450.

Interestingly, a unique fragment, assigned as T′ (T-H_2O; *m/z* 312 in Fig. 2(c)), is observed fairly abundantly in the spectrum of **F2a**, while the analogous ion in the spectrum of compound **F1a** (expected at *m/z* 314 in Fig. 2(b)) is barely detectable. It is logical to propose that dehydration of the T ion of compound **F2a** with elimination of the *N*-acyl 2′-hydroxy group is promoted by the adjacent Δ^3 unsaturation, yielding an *N*-2′,4′-octadecadienoate product, since it would be difficult to rationalize the difference in abundance of the T′ fragment in any other way. This effect may also influence the relative abundance of other ions derived from dehydration of primary fragments retaining the 2′-hydroxy fatty *N*-acyl group.

Application to CMH fractions from *Cryptococcus spp*

CMH fractions (**F3–F5**) were isolated from the yeastlike Basidiomycetes *Cr. laurentii*, *Cr. albidus*, and *Cr. neoformans* and found by HPTLC (comparison with standard fungal cerebrosides) and monosaccharide analysis (GC/MS of per-*O*-trimethylsilylated methyl glycosides, not shown) to contain glucose as the only sugar component. Figure 3 shows the $[M+Li]^+$ profiles of these cerebroside fractions. In addition to the predominant $[M + Li]^+$ at *m/z* 762 observed for the CMH of all three species (**F3a, F4, F5a**), minor components are observable at *m/z* 748 and 734 for the CMH of *Cr. laurentii* (**F3b, F3c**) and *Cr. neoformans* (**F5b, F5c**). Although these decrements of 14 and 28 Th from the mass of the major component could be assumed to correspond to differences in the fatty acyl moiety of 1 and 2 CH_2 units, respectively, other structural differences could also account for these mass intervals. In particular, the components at *m/z* 748 could be analogs lacking the 4,8-sphingadienine 9-methyl group, as was found previously for a glucocerebroside from *C. albicans*.[15] CID product ion spectra for the three $[M + Li]^+$ from *Cr. laurentii* CMH, reproduced in Fig. 4, confirmed that (i) the major component is identical in structure to the major CMH of the yeast form of *P. brasiliensis*, since the spectrum of **F3a** was essentially identical to that of **F1**, and (ii) the other two components indeed differ primarily by CH_2 units in the fatty acyl moiety, since their spectra are qualitatively similar, differing by 14 and 28 Th, respectively, only in those fragments which include the *N*-acyl group (base peak T ions

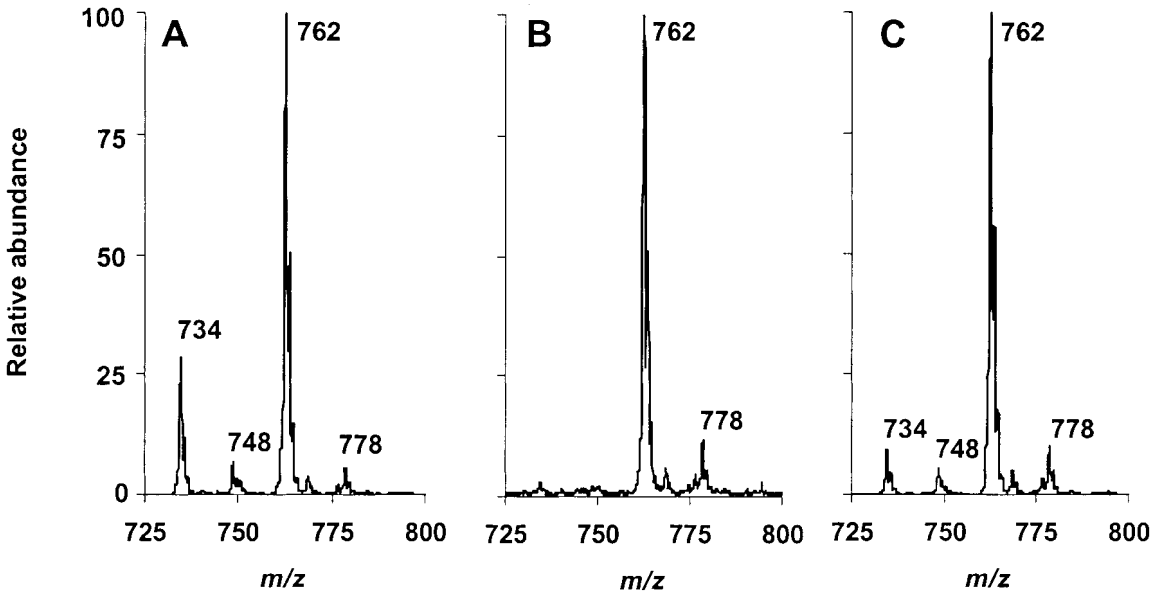

Figure 3. $^{+}$ESI-MS of cerebrosides from *Cryptococcus* spp. Pseudomolecular ion regions of $^{+}$ESI-MS spectra of CMHs from yeast forms of (a) *C. laurentii* (**F3**), (b) *C. albidus* (**F4**), and (c) *C. neoformans* (**F5**).

at *m/z* 318 and 304, W ions at *m/z* 247 and 233, for **F3b** and **F3c**). In the spectrum of the $[M + Li]^+$ at *m/z* 748, however, low abundance ions at *m/z* 494, 466, 448, 332, 304, and 261 are consistent with J, O, O′, T, N, and W fragments for an isobaric minor component lacking the sphingoid 9-methyl group. Similar results were obtained for these components in the *Cr. neoformans* CMH fraction (**F5a–F5c**). The cerebroside fractions from the three species appear to differ only in the relative amounts of the minor components. The results and assignments are summarized in Table 2.

It is worth nothing that attempts to obtain CID data from the Na^+ adduct of the h16:0 fatty acyl component required considerably more expenditure of material, either by increasing the number of scans or the concentration of the analyte. At best only the four major fragments could be observed (results not shown). It was not possible at all to obtain CID data from the Na^+ adduct of the h17:0 fatty acyl component. The comparative superiority of Li^+ adduction was clearly evident.

Application to CMH fractions from *Candida albicans* and *Aspergillus niger*

The method was next applied to characterization of a glucocerebroside extracted from the yeast form of *C. albicans* (**F6**). The major $[M + Li]^+$ was observed at *m/z* 762 (Fig. 5(a)), and $^{+}$ESI-MS/CID-MS of this component (**F6a**) yielded a spectrum (Fig. 6(a)) essentially identical to that of **F1a**, confirming the structure proposed in a previous report.[15] As with the *Cryptococcus* spp. described above, a minor component (**F6b**) was again observed at *m/z* 748. Although such a component was reported[15] to be an analog missing the 4,8-sphingadienine 9-methyl group, this CMH was obtained from a different strain of *C. albicans*, and, in the light of the alternative results obtained for the *Cryptococcus* CMHs with respect to CID analysis of *m/z* 748, it seemed that further investigation of this point by $^{+}$ESI-MS/CID-MS would be of interest. In fact the results in this case (Fig. 6(b)) confirmed that the 14 Th difference is for the most part not in the fatty acyl moiety but in the sphingoid base, as an abundant O ion is observed at *m/z* 466, while the T ion remains unshifted at *m/z* 332. Consistent with this, 14 Th shifts in all product ions retaining the entire sphingosine chain, but not the acyl chain, were observed, while any product ion derived from loss of all or part of the sphingosine chain including C8 remained unshifted (Table 2). Interestingly, it is possible to detect in this CID spectrum some very low abundance O, T, and W ions at *m/z* 480, 318, and 247, respectively, indicating an extremely minor component in which the mass difference resides in the fatty acyl moiety (h17:0 fatty acid + d19:2 sphingoid).

Investigation of the even less abundant $[M + Li]^+$ at *m/z* 734 (Fig. 5(a)) by $^{+}$ESI-MS/CID-MS was possible, although the analysis was complicated by low overall signal-to-noise, and by detection of product ions consistent with four isobaric components, one of which was not a cerebroside (results not shown). Nevertheless, the major fragments characteristic for three isobaric cerebrosides could be clearly observed. Along with Y_0, C_1, and β_1 ions at *m/z* 572, 187, and 169, respectively, three pairs of T and O ions were observed at *m/z* 304 and 480, *m/z* 318 and 466, and *m/z* 332 and 452, consistent with cerebrosides having fatty acyl/sphingoid combinations h16:0/d19:2, h17:0/d18:2, h18:0/d17:2, respectively.

The $[M + Li]^+$ profile of a cerebroside extracted from *A. niger* (**F7**) is compared in Fig. 5(b) with that from *C. albicans* (Fig. 5(a)). In $^{+}$ESI-MS profile mode, the Li^+ adduct of the *A. niger* cerebroside (**F7**) was observed abundantly and almost exclusively at *m/z* 760; the ion abundance at *m/z* 762 appeared to be approximately double that expected for the + 2 ^{13}C isotope peak of the *m/z* 760 component (Fig. 5(b)). $^{+}$ESI-MS/CID-MS of the *m/z* 760 ion yielded a spectrum (Fig. 7(a)) essentially identical to that of compound **F2a** (h18:1/d19:2). A similar analysis selecting *m/z* 762 as precursor yielded a complex spectrum corresponding to the expected result from a mixture of **F1a** and the + 2 isotope peak of **F2a** (not shown). Since a monosaccharide analysis of the *A. niger* cerebroside (GC/MS of per-*O*-trimethylsilylated methyl glycosides) yielded mainly glucose, with a small amount of galactose

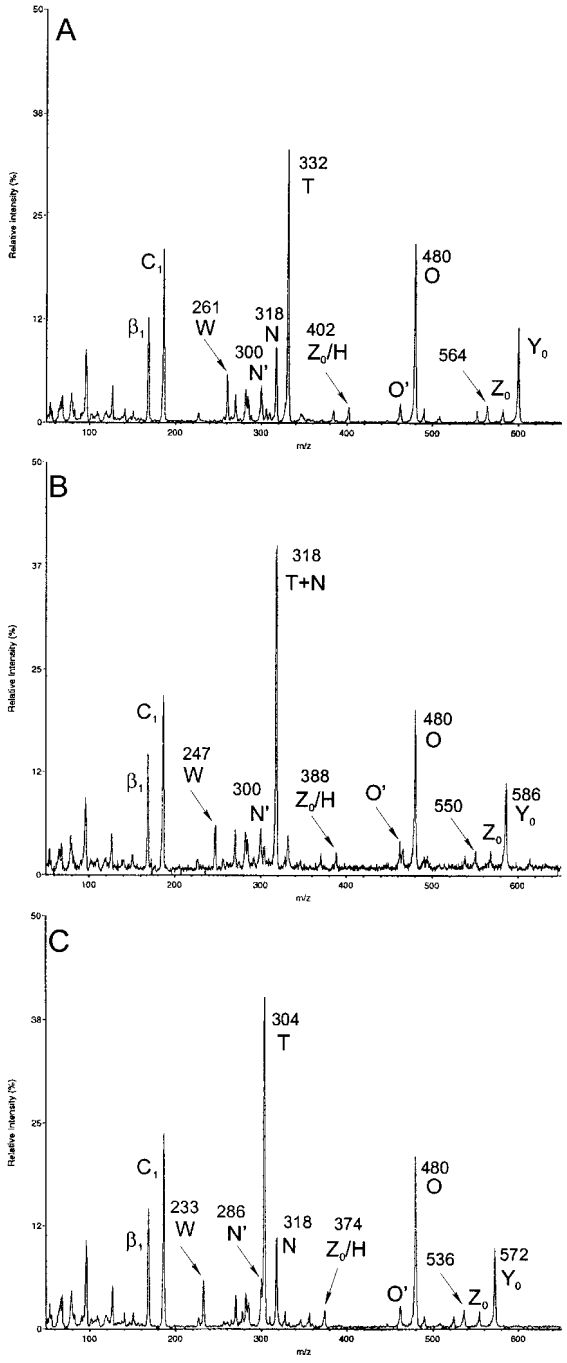

Figure 4. Tandem $^{+}$ESI-MS/CID-MS product ion spectra from $[M + Li]^{+}$ from *C. laurentii* cerebroside fraction (**F3**). Tandem $^{+}$ESI-MS/CID-MS product ion spectra from $[M + Li]^{+}$ of *C. laurentii* yeast form CMH components (a) **F3a**, *m/z* 762; (b) **F3b**, *m/z* 748; and (c) **F3c**, *m/z* 734.

(5–10%), it could be concluded that the major component (**F7a**) is a glucocerebroside having a ceramide identical to that of **F2a**. This is contrary to a previous report[35] that a cerebroside extracted from *A. niger* consisted exclusively of galactose attached to ceramides containing d18:1 sphing-4-enine and d18:0 sphinganine, although the identification of the major fatty acyl component as a 2′-hydroxyoctadecenoate (position of unsaturation unspecified) was correct. Our proposed composition for the major CMH component of *A. niger* (**F7a**) was confirmed by ^{1}H-NMR spectroscopy (S.B. Levery and R.L. Doong, unpublished results).

As with the *Cryptococcus* and *C. albicans* glucocerebrosides, it was also possible to analyze minor $[M + Li]^{+}$ components in the *A. niger* CMH profile by $^{+}$ESI-MS/CID-MS. Products of *m/z* 746 (Fig. 7(b)) were again consistent with the absence of the sphingoid 9-methyl group in the bulk of this component (**F7b**), with abundant O and T ions observed at *m/z* 466 and 330, respectively. Consistent 14 Th shifts were again observed in all product ions retaining the entire sphingosine chain, but not the acyl chain (Table 2). Lower abundance O, T, T′, and W ions were observed at *m/z* 480, 316, 298, and 245, respectively, consistent with a minor component having h17:1 fatty acid and d19:2 sphingoid. Products of *m/z* 732 (not shown) were similarly consistent with the presence of three cerebroside components, exhibiting T + O pairs at *m/z* 302 + 480 (h16:1/d19:2), *m/z* 316 + 466 (h17:1/d18:2), and *m/z* 330 + 452 (h18:1/d17:2).

Analysis of minor components of CMH fractions from yeast and mycelium forms of *Paracoccidiodes brasiliensis*

During a previous study of cerebrosides extracted from *P. brasiliensis*,[22] which utilized $^{+}$ESI-MS/CID-MS of Na^{+} adduct ions, it was not practical to analyze such minor components as described above. The superior efficacy of $^{+}$ESI-MS/CID-MS with Li^{+} cationization prompted us to reexamine in more detail the CMH fractions from both yeast and mycelium forms of *P. brasiliensis*. This led to identification of additional structural variants providing further details about cerebroside biosynthesis in this fungus. The $[M + Li]^{+}$ profiles of *P. brasiliensis* yeast and mycelium form glucocerebroside fractions (Figs 8(a) and (b), respectively) reflect the much lower proportion of (*E*)-Δ^3 unsaturation of the 2-hydroxy fatty acyl moiety in the former, as manifested by the much lower abundance of *m/z* 760 relative to *m/z* 762. The structure and CID spectrum of the major yeast form CMH component (**F1a**; *m/z* 762) have already been discussed above. The CID spectrum of the *m/z* 762 component in the mycelium form CMH is essentially identical to that of **F1a**, while the CID spectrum of the *m/z* 760 component (**F8a**) is essentially the same as that of **F2a**, in agreement with previous results using Na^{+} adduct ions.[22]

Of interest here are the lower abundance $[M + Li]^{+}$ species, such as those observed at *m/z* 790, 750, 748, and 734 in the yeast and mycelium form CMH spectra (Fig. 8(a,b)), and the additional species at *m/z* 746 and 732 observed in the mycelium form CMH spectrum (Fig. 8(b)). A CID spectrum of the $[M + Li]^{+}$ at *m/z* 790 (Fig. 9(a)) in the yeast form CMH profile appears characteristic for a fungal cerebroside homolog (**F1g**) having the dominant d19:2 sphingoid in combination with h20:0 fatty acid (O, T and W ions at *m/z* 480, 360, and 289, respectively). There is scant evidence for an isobaric h18:0/d21:2 fatty acyl/sphingoid component; in the absence of significant abundance at *m/z* 332 (T) or *m/z* 261 (W), the ion at *m/z* 508 is assigned exclusively as the J fragment from **F1g** with no significant contribution from an O fragment, *m/z* 480 + 28. On the other hand, though a similar spectrum was obtained from the corresponding mycelium form component (**F8g**; not shown), lower abundance ions could also be observed at *m/z* 510, 330, and 259, consistent with O, T and W fragments from an isobaric h18:1/d21:1 minor component.

Unlike the $[M + Li]^{+}$ profiles considered previously, in

Table 2. $^{+}$ESI-MS/CID-MS data (all fragments $^{\cdot}Li^{+}$ except where noted) for cerebroside components from *Cr. laurentii* (F3a–F3c), *Cr. albidus* (F4a), and *Cr. neoformans* (F5a–F5c); *C. albicans* (F6a, F6b); and *A. niger* (F7a, F7b); with proposed interpretations of fragments (all values nominal, monoisotopic *m/z*). Fragment nomenclature is after Costello *et al.*[25,28,34] as modified and expanded by Adams and Ann[26] (see Scheme 2). 3–5 most abundant fragments in each spectrum are in boldface

	F3a **F4a** **F5a**	**F3b** **F5b**	**F3c** **F5c**	**F6a**	**F6b**	**F7a**	**F7b**
Fatty acid:	h18:0	h17:0	h16:0	h18:0	h18:0	h18:1	h18:1
Sphingosine:	d19:2	d19:2	d19:2	d19:2	d18:2	d19:2	d18:2
M	762	748	734	762	748	760	746
Y_0	600	586	572	600	586	598	584
Z_0	582	568	554	582	568	580	566
Z_0' ($\equiv Z_0$–H_2O)	564	550	536	564	550[a]	562	548
H′ ($\equiv$ H–H_2O)	564	550	536	564	564	562	562
Z_0–CH_2O	552	538	524	552	538	550	536
J ($\equiv$ M–acyl C_2-C_ω)	508	508	508	508	494	508	494
J′ ($\equiv$ J–H_2O)	490	490	490	490	476	490	476
O ($\equiv$ M–acyl)	**480**	**480**	**480**	**480**	**466**	**480**	**466**
O′ ($\equiv$ M–acyl-H_2O)	462	462	462	462	448	462	448
Z_0/H	402	388	374	402	402	400	400
Z_0/H′ ($\equiv Z_0$/H–H_2O)	384	370	356	384	384	382	382
Z_0/H″ ($\equiv Z_0$/H–$2H_2O$)	—	—	—	—	—	364	364
S ($\equiv Y_0$/G)	348	334	320	348	348	346	346
T ($\equiv Z_0$/G)	**332**	**318**	**304**	**332**	**332**	**330**	**330**
N ($\equiv Y_0$/O)	318	318	318	318	304	318	304
T′ ($\equiv$ T–H_2O)	314[a]	300[b]	286[a]	314[a]	314[a]	312	312
U ($\equiv$ T–C_2H_2)	306	292	278	306	306	304	304
N′	300	300	300	300	286	300	286
N″ [Li^+]	282	282	282	282	268	282	268
N″ [H^+]	—	—	—	—	—	—	—
N′–CH_2O	270	270	270	270	256	270	256
W (acyl C_2-C_ω)	261	247	233	261	261	259	259
E	228	228	228	228	228	228	228
C_1	**187**	**187**	**187**	**187**	**187**	**187**	**187**
β_1	**169**	**169**	**169**	**169**	**169**	**169**	**169**
$^{0,2}A_1$	127	127	127	127	127	127	127
$^{0,2}A_1$–CH_2O	97	97	97	97	97	97	97

[a] Very weak.

[b] Probably does not contribute significantly to abundance of this fragment (isobaric with more abundant fragment in spectrum).

the *P. brasiliensis* yeast and mycelium form CMH spectra the *m/z* 750 species are clearly more abundant than expected if they represented solely the + 2 isotope peak of the *m/z* 748 components. The CID spectrum of the yeast form CMH *m/z* 750 ion (Fig. 9(b)) is consistent with a cerebroside analog (**F1b**) having 2-hydroxyoctanoate and missing both the sphingoid 9-methyl group and the Δ^8 unsaturation, yielding an O ion at *m/z* 468 and a T ion at *m/z* 332. Consistent with saturation of the sphingosine from C6 on, the N ion at *m/z* 306 is again more abundant than the T ion, as was observed with the bovine brain galactocerebrosides having d18:1 sphingosine and 2-hydroxy fatty acylation (e.g., **B2a-c**). The Y_0 ion, *m/z* 588, is again the fourth most abundant ion in the CID spectrum. Overall, the CID spectrum was essentially indistinguishable from that of compound **B2c**, also having h18:0 fatty acid (*m/z* 750; see Table 1), including the *m/z* and relative abundance of the minor fragments.

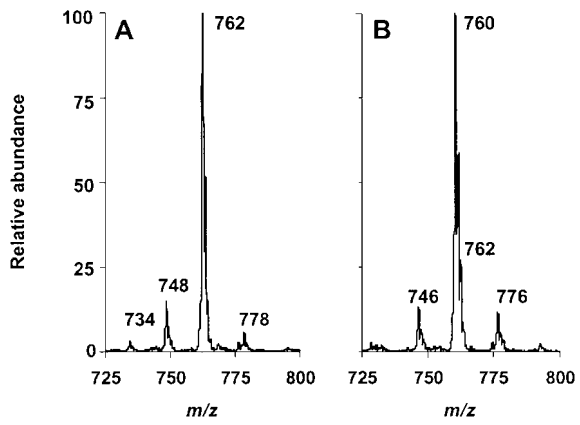

Figure 5. $^{+}$ESI-MS of cerebroside fractions extracted from yeast form of *C. albicans* and from mycelia of *A. niger*. Pseudomolecular ion regions of $^{+}$ESI-MS spectra of CMH fractions from (a) *C. albicans* (**F6**) and (b) *A. niger* (**F7**).

The CID spectrum of the *m/z* 748 ion (not shown; see Table 3) also presented a somewhat different result from those observed previously with either *Cryptococcus* spp. (**F3b, F5b**), or *C. albicans* (**F6b**), exhibiting fragments characteristic of *both* h17:0/d19:2 (**F1c1**) and h18:0/d18:2 (**F1c2**) fatty acyl/sphingoid species in comparable abundances. The two species are represented by O + T pairs at *m/z* 480 + 318 and *m/z* 466 + 332, respectively, while the N ions are at *m/z* 318 and 304, respectively (of which the former is not distinguishable from the corresponding T ion). On the other hand, the CID spectrum of the *m/z* 734 ion (not shown; Table 3) is characteristic mainly of a single species having an h16:0/d19:2 (**F1e**) fatty acyl/sphingoid combination (O + T pair at *m/z* 480 + 304). A low abundance O + T pair at *m/z* 452 and 332 is consistent with the presence of a

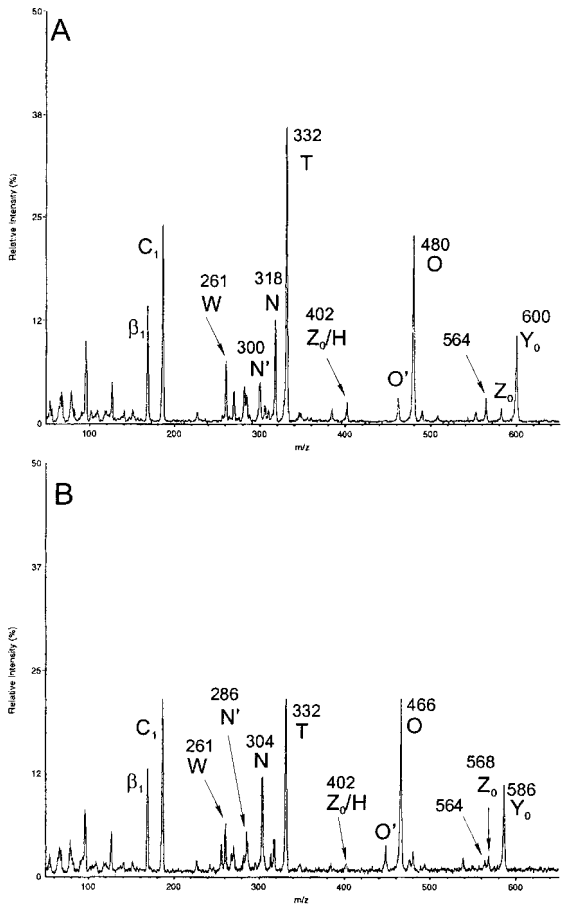

Figure 6. Tandem $^{+}$ESI-MS/CID-MS product ion spectra of $[M + Li]^{+}$ from *C. albicans* cerebroside fraction (**F6**). (a) Major pseudomolecular ion, *m/z* 762 (**F6a**) and (b) minor pseudomolecular ion, *m/z* 748 (**F6b**).

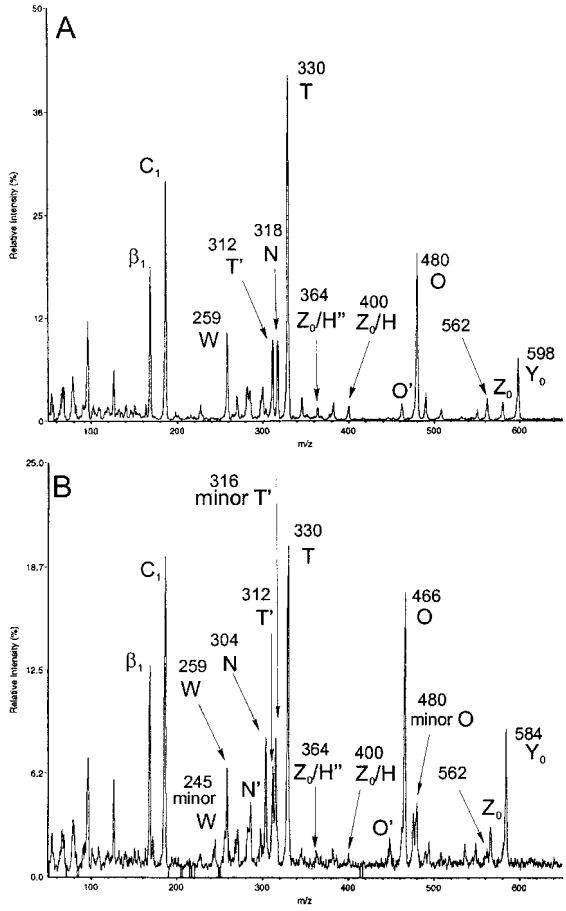

Figure 7. Tandem $^{+}$ESI-MS/CID-MS product ion spectra from $[M + Li]^{+}$ of *A. niger* cerebroside fraction (**F7**). (a) Major pseudomolecular ion, *m/z* 760 (**F7a**) and (b) minor pseudomolecular ion, *m/z* 746 (**F7b**).

small amount of an h18:0/d17:2 fatty acyl/sphingoid combination.

The CID spectra from the *m/z* 750, 748, and 734 ions in the *P. brasiliensis* mycelium form CMH profile (**F8b, F8c1/c2, F8e**; not shown) were essentially identical to those from the yeast form, except that fragments from an additional component (**F8c3**) were present in the *m/z* 748 spectrum. These were consistent with an analog of the *m/z* 750 component having Δ^3 unsaturation, h18:1/d18:1 (additional O + T pair at *m/z* 468 + 330; abundant N fragment at *m/z* 306; T′ fragment at *m/z* 312; additional W fragment at *m/z* 259). An additional difference in the mycelium form *m/z* 734 was the absence of an observable O + T pair at *m/z* 332 and 452 corresponding to the trace h18:0/d17:2 fatty acyl/sphingoid component seen in the yeast form.

The CID spectrum from *m/z* 746 in the *P. brasiliensis* mycelium form profile (not shown), in contrast to that of *m/z* 748 from both forms, represented mainly a single species having the h18:1/d18:2 (**F8d**) fatty acyl/sphingoid combination (O + T pair at *m/z* 466 + 330). A minor component having the h17:1/d19:2 fatty acyl/sphingoid combination (O + T pair at *m/z* 480 + 316) was observed at low abundance. The CID spectrum from *m/z* 732 in the *P. brasiliensis* mycelium form profile (not shown), similar to that of *m/z* 734 from both forms, represented essentially a single species having the additionally unsaturated h16:1/d19:2 (**F8f**) fatty acyl/sphingoid combination (O + T pair at *m/z* 480 + 302). These results, along with additional supporting minor fragments, are summarized in Table 3.

DISCUSSION

The use of Li^{+} cationization with tandem quadrupole $^{+}$ESI-MS/CID-MS of cerebrosides yielded a substantial increase in observable fragmentation compared with spectra obtained from sodiated species acquired under comparable conditions. The tandem quadrupole CID spectra of lithiated cerebrosides differed substantially from those obtained at high energies, particularly in the absence of fragments at *m/z* above that of Y_0. These high *m/z* fragments represent for the most part consecutive cleavages of the distal alkyl and acyl CH_2 chains, and their usefulness will vary depending on whether remote functional groups are present.[26] So far, these have not been found in fungal cerebrosides, but the possibility should not be discounted when new species are examined. Some other useful fragments found in higher energy CID modes were not observed, but major fragments which allow differences in molecular mass to be assigned to either the fatty acyl or sphingosine moiety were well represented. In addition, the low energy CID spectra of lithiated cerebrosides exhibited a number of low-to-medium abundance fragments, not previously observed with sodiated cerebrosides,[22] which appear to be reliable indicators of specific ceramide structural modifications, including

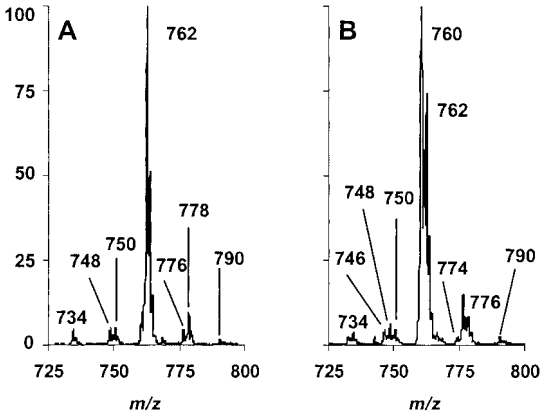

Figure 8. $^{+}$ESI-MS of glucocerebroside fractions extracted from yeast and mycelium forms of *P. brasiliensis*. Pseudomolecular ion regions of $^{+}$ESI-MS spectra of CMH fractions from (a) yeast form (**F1**) and (b) mycelium form (**F8**).

fatty acyl 2-hydroxylation and Δ^3 unsaturation, and sphingoid base Δ^8 unsaturation. These are all structural features commonly found in fungal cerebrosides. The presence or absence of a characteristic sphingoid branching 9-methyl group can also be determined, although its location on the alkyl chain is not inherently specified by the fragmentation observed in this mode, except that it is clearly excluded from carbons 4–8. This feature is readily assigned by NMR spectroscopy,[22] but it is worth noting that NMR is not useful for establishing either the absolute or relative lengths of the alkyl and acyl chains in a ceramide, since the bulk of mid-chain alkyl/acyl CH_2 groups resonate at a single frequency. On the other hand, such chain length assignments are conveniently obtained from MS/CID-MS experiments.

A nearly tenfold increase in overall signal-to-noise was a second major advantage observed for Li^+ over Na^+ cationization in CID experiments. This enabled us to determine details of ceramide structure of cerebroside components present at far less than 5% of the abundance of the major component(s), even where minor molecular ion peaks contained multiple components. For many of these minor components, we were previously unable to detect even the most abundant fragments expected when Na^+ cationization was used. Note that the analyte concentrations and the number of scans accumulated per spectrum were often higher than necessary in this study, in order to assure acquisition of a full set of fragments from as many components as possible. Useful spectra could be obtained routinely from minor components present at levels as low as ~1% of the major component, or 0.2 ng/μL (~0.25 pmol/μL), at a flow rate of 3 μL/min after a period of 10 minutes (~60 scans, although more were frequently accumulated). This translates to an expenditure of ~7–8 pmol for each minor component. While this is hardly spectacular, it was achieved without rigorous optimization of sensitivity, as we were not sample limited for these particular cerebrosides.

Besides differences between fungi which were obvious from analysis of the major components (e.g., between the glucocerebroside of *A. niger*, which contains a high proportion of 2-hydroxy fatty acyl (*E*)-Δ^3 unsaturation, and that of *C. albicans*, which contains only fully saturated 2-hydroxy fatty acid), examination of the minor components revealed differences between fungi even where the major

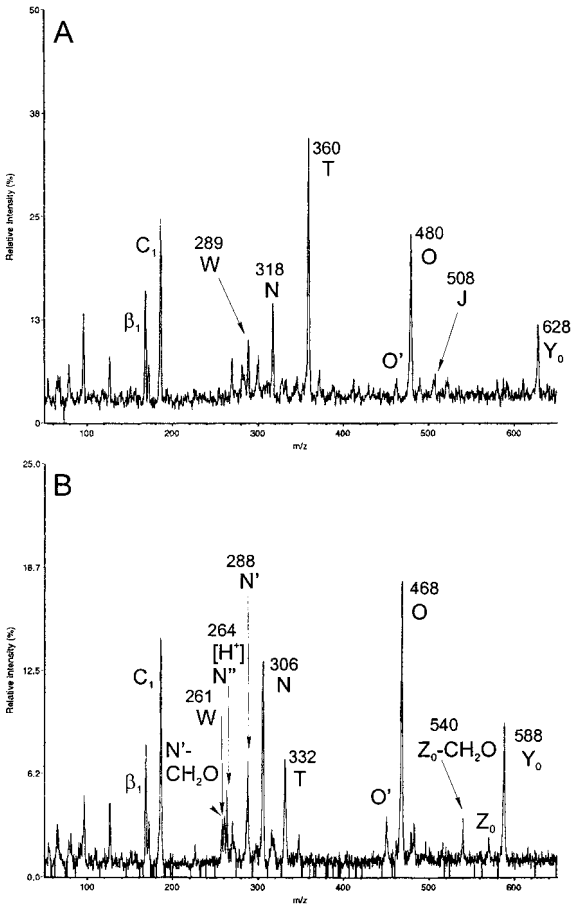

Figure 9. Tandem $^{+}$ESI-MS/CID-MS product ion spectra from minor pseudomolecular ions $[M + Li]^+$ of yeast form *P. brasiliensis* glucocerebroside fraction (**F1**). (a) *m/z* 790 (**F1g**) (300 scans accumulated) and (b) *m/z* 750 (**F1b**).

components were identical (e.g., between the glucocerebroside of *C. albicans*, which contains detectable components lacking the sphingoid branching 9-methyl group, and those of *Cryptococcus* spp., for which this component was barely observed). Since minor variants lacking the 9-methyl group and/or Δ^8 unsaturation are most likely biosynthetic intermediates, the relative abundance of these components, or of fatty *N*-acyl homologous series, could provide clues to differences in activity and/or specificity of homologous enzymes employed for cerebroside biosynthesis in various fungi. Thus far (including the results in this study), it appears that the (*E*)-Δ^3 unsaturation of the 2′-hydroxy fatty *N*-acyl group is confined to Euascomycetes (e.g., *P. brasiliensis*, *Aspergillus* spp.), and has not been found in cerebrosides of Basidiomycetes (e.g., *Agaricus* spp., *Cryptococcus* spp.) or Hemiascomycetes (e.g., *C. albicans*). On the other hand, variation of 2′-hydroxy fatty *N*-acyl chain length appears to be more significant in cerebrosides of Basidiomycetes, and more tightly regulated in many Euascomycetes and in *C. albicans*. At present the functional significance for such variations remains unclear, but it has been suggested that cerebrosides could play a role in membrane signaling cascades regulating morphogenesis in thermally dimorphic mycopathogens.[22] The dimorphism observed in the level of (*E*)-Δ^3 unsaturation between the yeast and mycelial forms of *P. brasiliensis* may be relevant to this hypothesis.

The ability to detect a wide variety of structural

Table 3. $^{+}$ESI-MS/CID-MS data (all fragments •Li^{+} except where noted) for *P. brasiliensis* yeast form glucocerebroside (minor components, F1b, F1c1, F1c2, F1e, F1g) and mycelium form glucocerebroside (minor components, F8b, F8c1–3, F8d–g) with proposed interpretations of fragments (all values nominal, monoisotopic *m/z*). Fragment nomenclature is after Costello *et al.*[25,28,34] as modified and expanded by Adams and Ann[26] (see Scheme 2). 3–5 most abundant fragments in each spectrum are in boldface

	F1g F8g	**F1b F8b**	**F1c1 F8c1**	**F1c2 F8c2**	**F8c3**	**F8d**	**F1e F8e**	**F8f**
Fatty acid:	h20:0	h18:0	h17:0	h18:0	h18:1	h18:1	h16:0	h16:1
Sphingosine:	d19:2	d18:1	d19:2	d18:2	d18:1	d18:2	d19:2	d19:2
M	790	750	748	748	748	746	734	732
Y_0	628	**588**	586	586	586	584	572	570
Z_0	610	570	568	568	568	566	554	552
Z_0'(≡ Z_0–H_2O)	592	—	550	550	550	548	536	534
H′ (≡ H–H_2O)	592	—	550	564	—	562	536	534
Z_0–CH_2O	580	540	538	538	538	536	524[a]	522
J (≡ M–acyl C_2-C_ω)	508	496[a]	508	494	496[a]	494	508	508
J′ (≡ J–H_2O)	490	478	490	476	478	476	490	490
O (≡ M–acyl)	**480**	**468**	**480**	**466**	**468**	**466**	**480**	**480**
O′ (≡ M–acyl–H_2O)	462	450	462	448	450	448	462	462
Z_0/H	430	402[a]	388	402	400	400	374	372
Z_0/H′ (≡Z_0/H–H_2O)	412	—	370	384	382	382	356	354
Z_0/H″ (≡Z_0/H–2H_2O)	—	—	—	—	364	364	338[a]	336
S (≡ Y_0/G)	376	348	334	348	346	346	320	318[b]
T (≡ Z_0/G)	**360**	332	**318**	**332**	330	**330**	**304**	**302**
N (≡ Y_0/O)	318	**306**	318	304	**306**	304	318	318
T′ (≡ T–H_2O)	342[a]	314[a]	300[b]	314[a]	312	312	286[a]	284
U (≡ T–C_2H_2)	334	306[b]	292	306	304	304	278	278
N′	300	288	300	286	288	286	300	300
N″ [Li^{+}]	282	270	282	268	270	268	282	282
N″ [H^{+}]	—	264	—	—	264	—	—	—
N′–CH_2O	270	258	270	256	258	256	270	270
W (acyl C_2-C_ω)	289	261	247	261	259	259	233	231
E	228	228	228	228	228	228	228	228
C_1	**187**	**187**	**187**	**187**	**187**	**187**	**187**	**187**
β_1	**169**	**169**	**169**	**169**	**169**	**169**	**169**	**169**
$^{0,2}A_1$	127	127	127	127	127	127	127	127
$^{0,2}A_1$–CH_2O	97	97	97	97	97	97	97	97

[a] Very weak.
[b] Probably does not contribute significantly to abundance of this fragment (isobaric with more abundant fragment in spectrum).

variations should prove very useful in characterizing mutations in cerebroside biosynthesis, where one or more of the characteristic ceramide modifying enzymes could be deleted. We anticipate being able to use this approach to confirm the effect of gene insertions or inactivations on cerebroside structure, with a view toward establishing functional correlations between CMH structural alterations and fungal phenotypes or changes in morphology. In this connection it is worth emphasizing that simply profiling CMH molecular ions, whether directly on purified fractions or by parent ion scanning of a common precursor in crude lipid mixtures,[29] may be insufficient in certain cases for full characterization. Since isobaric molecular species can be produced by a variety of distinct structural modifications, as illustrated by several cases in the present study, the use of CID experiments is essential. The ability for some species to produce both GlcCer and GalCer[13,22,36] is a further complication, particularly since they may be expressed with substantially different levels of (*E*)-Δ^3 unsaturation.[22] In such cases, some form of prior fractionation would be an additional requirement for complete characterization of CMH fractions, and, ideally, the analysis would be performed via direct HPLC interface, using a more sensitive state-of-the-art instrument designed for rapid scanning and automated acquisition of CID spectra.

Acknowledgements

This work was supported by FAPESP, CNPq, and PRONEX (Brasil; M.S.T., A.H.S., and H.K.T.), a Glycoscience Research Award from Neose Technologies, Inc. (S.B.L.), and the National Institutes of Health Resource Center for Biomedical Complex Carbohydrates (NIH #5 P41 RR05351; S.B.L.).

REFERENCES

1. Kanfer JN, Hakomori S. *Sphingolipid Biochemistry*, Plenum Press; New York, 1983.
2. Jin W, Rinehart KL, Jares-Erijman EA. *J. Org. Chem.* 1994; **59**: 144.
3. Natori T, Morita M, Akimoto K, Koezuka Y. *Tetrahedron* 1994; **50**: 2771.
4. Karlsson K-A, Leffler H, Samuelsson BE. *Biochim. Biophys. Acta* 1979; **574**: 79.
5. Costantino V, Fattorusso E, Mangoni A. *Liebigs Ann.* 1995; 1471.
6. Costantino V, Fattorusso E, Mangoni A. *Liebigs Ann.* 1995; 2133.
7. Shibuya H, Kawashima K, Sakagami M, Kawanishi H, Shimomura M, Ohashi K, Kitagawa T. *Chem. Pharm. Bull. (Tokyo)* 1990; **38**: 2933.
8. Ballio A, Casinovi CG, Framondino M, Marino G, Nota G, Santurbano B. *Biochim. Biophys. Acta* 1979; **573**: 51.
9. Fujino Y, Ohnishi M. *Biochim. Biophys. Acta* 1976; **486**: 161.
10. Sitrin RD, Chan G, Dingerdissen J, DeBrosse C, Mehta R, Roberts G, Rottschaefer S, Staiger D, Valenta J, Snader KM, Stedman RJ, Hoover JRE. *J. Antibiot. (Tokyo)* 1988; **41**: 469.
11. Sawabe A, Morita M, Okamoto T, Ouchi S. *Biol. Mass Spectrom.* 1994; **23**: 660.

12. Fogedal M, Mickos H, Norberg T. *Glycoconjugate J.* 1986; **3**: 233.
13. Villas Boas MH, Egge H, Pohlentz G, Hartmann R, Bergter EB. *Chem. Phys. Lipids* 1994; **70**: 11.
14. Duarte RS, Polycarpo CR, Wait R, Hartmann R, Bergter EB. *Biochim. Biophys. Acta* 1998; **1390**: 186.
15. Matsubara T, Hayashi A, Banno Y, Morita T, Nozawa Y. *Chem. Phys. Lipids* 1987; **43**: 1.
16. Kawai G, Ikeda Y. *J. Lipid Res.* 1985; **26**: 338.
17. Kawai G, Ikeda Y. *Biochim. Biophys. Acta* 1983; **754**: 243.
18. Kawai G, Ikeda Y. *Biochim. Biophys. Acta* 1982; **719**: 612.
19. Mizushina Y, Hanashima L, Yamaguchi T, Takemura M, Sugawara F, Saneyoshi M, Matsukage A, Yoshida S, Sakaguchi K. *Biochem. Biophys. Res. Commun.* 1998; **249**: 17.
20. Kawai G, Ikeda Y, Tubaki K. *Agric. Biol. Chem.* 1985; **49**: 2137.
21. Koga J, Yamauchi T, Shimura M, Ogawa N, Oshima K, Umemura K, Kikuchi M, Ogasawara N. *J. Biol. Chem.* 1998; **273**: 31985.
22. Toledo MS, Levery SB, Straus AH, Suzuki E, Momany M, Glushka J, Moulton JM, Takahashi HK. *Biochemistry* 1999; **38**: 7294.
23. Dell A. *Adv. Carbohydr. Chem. Biochem.* 1987; **45**: 19.
24. Egge H, Peter-Katalinic J. *Mass Spectrom. Rev.* 1987; **6**: 331.
25. Costello CE, Vath JE. *Methods Enzymol.* 1990; **193**: 738.
26. Adams J, Ann Q. *Mass Spectrom. Rev.* 1993; **12**: 51.
27. Peter-Katalinic J. *Mass Spectrom. Rev.* 1994; **13**: 77.
28. Domon B, Costello CE. *Biochemistry* 1988; **27**: 1534.
29. Gu M, Kerwin JL, Watts JD, Aebersold R. *Anal. Biochem.* 1997; **244**: 347.
30. Ann Q, Adams J. *J. Am. Soc. Mass Spectrom.* 1992; **3**: 260.
31. Ann Q, Adams J. *Anal. Chem.* 1993; **65**: 7.
32. Sullards MC, Schmelz E-M, Merrill AH. Jr. *Proc. 46th ASMS Conf. Mass Spectrom. Allied Top.* 1998; 661.
33. Olling A, Breimer ME, Samuelsson BE, Ghardashkhani S. *Rapid. Commun. Mass Spectrom.* 1998; **12**: 637.
34. Domon B, Vath JE, Costello CE. *Anal. Biochem.* 1990; **184**: 151.
35. Wagner H, Fiegert E. *Z. Naturforsch. B* 1969; **24**: 359.
36. Toledo MS, Levery SB, Straus AH, Takahashi H. *J. Lipid Res.*, 2000; in press.

